Role of charge-resonance states in liquid high-order harmonic generation

Chang-Long Xia,[1,2] Zheng-Liang Li,[1,3] Jia-Qi Liu,[1,3] Ai-Wu Zeng,[1,3] Ling-Jie Lü,[1,3] and Xue-Bin Bian[1,*]

[1]*State Key Laboratory of Magnetic Resonance and Atomic and Molecular Physics, Wuhan Institute of Physics and Mathematics, Innovation Academy for Precision Measurement Science and Technology, Chinese Academy of Sciences, Wuhan 430071, China*

[2]*College of Physics and Information Engineering, Shanxi Normal University, Taiyuan 030031, China*

[3]*School of Physical Sciences, University of Chinese Academy of Sciences, Beijing 100049, China*

(Received 23 March 2021; revised 28 July 2021; accepted 7 January 2022; published 24 January 2022)

High-order harmonics can be generated in the gas, solid, plasma, and liquid samples driven by intense ultrafast lasers. The microscopic mechanisms of the former three have been well studied. However, liquid high-order harmonic generation (HHG) has demonstrated many unexpected results compared to other materials. Due to the complexity of liquids, it is still unknown what the quantum origin of the liquid HHG is. Here we reveal the role of localized charge-resonance states in HHG from disordered liquids. A quantum theory based on statistical two-level resonance is developed, which explains well almost all the characters of liquid harmonics known so far, such as the cutoff energy independence of wavelength. It may shed light on the optimal control of harmonic generation in liquids.

DOI: 10.1103/PhysRevA.105.013115

I. INTRODUCTION

Laser technology provides us a powerful tool for studying ultrafast physics [1], such as tunneling ionization [2–4], high-order harmonic generation (HHG) [5–7], and so on. HHG can be utilized as not only coherent attosecond pulse sources, but also probes for extracting ultrafast dynamic information of the microworld with high spatial and temporal resolutions [8]. To achieve this, people have to construct physical models to describe the mechanisms of HHG. For the gas-phase HHG, the recollision model is well accepted [6]. For the solid-phase HHG, intra- and interband transitions are thought of as the sources [9,10]. For the HHG in plasma, the coherent wake emission and the relativistic oscillating mirror mechanisms are identified [11]. The electron dynamics in liquids which link physics with the chemical reactions and biological processes are very important. Recently, HHG from liquids has been studied experimentally [12–14]. For bulk liquids driven by monochromatic fields, it is found that the cutoff energy is proportional to the electric field strength E_0 of the laser [14,15], but independent on the driving laser wavelength [15]. This character is quite different from that in the gas and solid HHG, which has attracted much attention recently. However, the liquid system is rather complex. Even the most common water has a lot of anomalous properties, such as the law of density with temperature. The microscopic mechanism of liquid HHG is still a mystery.

In the theoretical aspect, a statistical random model chain is used to simulate the liquid HHG processes [15]. The radial distribution function of a liquid could be reproduced. By taking consideration of the statistical effect, an empirical cutoff formula for the nonperturbative HHG in monochromatic fields is obtained,

$$\Omega = E_0 d^* = \frac{E_0 a(a-\sigma)}{\sigma}, \tag{1}$$

where a is the average distance, σ is the standard deviation, and d^* is the maximum coherence distance. Although the formula based on classical physics is consistent with the experimental results of the linear cutoff law on E_0, the quantum micromechanisms behind liquid HHG are still unknown. For the gas-phase HHG, the cutoff energy is proportional to A_0^2 [6]. For crystal HHG, some works find that the cutoff energy is related to A_0 [16–19], while some works think that it is only determined by E_0 rather than λ [20]. It may come from the multielectron effect or the dominance of intraband currents. However, the physics behind the cutoff independence of wavelength in liquid systems is still not clear. Based on Eq. (1), the cutoff energy in liquid HHG in a two-color laser scheme [21,22] should depend on the peak effective field strength of the superposed fields. However, we find that the results are unexpected. By numerical solutions of the time-dependent Schrödinger equations (TDSEs), the HHG cutoff energy only changes slightly even though the superposed field strength E' is apparently increased when the phase $\varphi = 0$. The cutoff decreases obviously even if the effective field strength E' is very close to the monochromatic field when $\varphi = \pi$. A quantum version explanation based on mathematical derivations is highly desired to explain the wavelength-independent cutoff in monochromatic fields and the break of linear field-strength-dependent cutoff law in bichromatic fields. In this paper, we developed a statistical two-level resonance model, which can interpret the origin of the characters of liquid HHG in the monochromatic and bichromatic laser fields.

II. NUMERICAL SIMULATIONS

The details of the numerical TDSE method can be found in Ref. [15]. For a given σ, we perform several calculations

*xuebin.bian@wipm.ac.cn

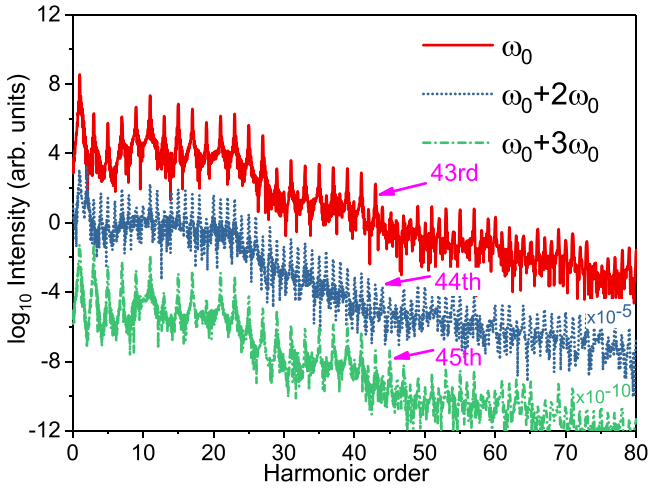

FIG. 1. High-order harmonic spectra from one-color and two-color laser schemes. The laser parameters are in the main text. A trapezoidal envelope with full width at half maximum of $10T_0$ is used.

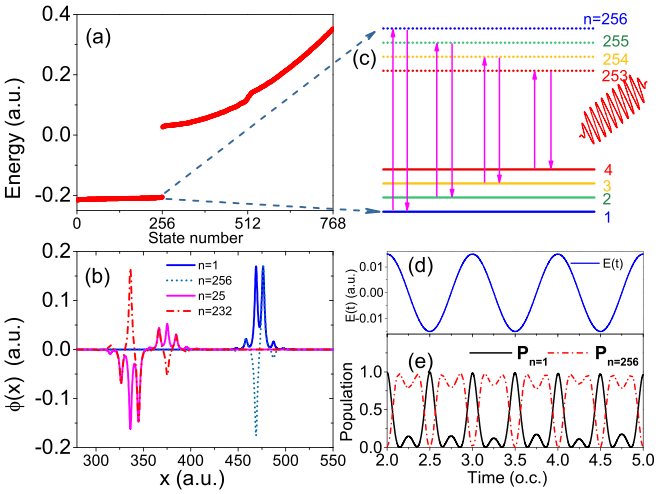

FIG. 2. (a) The eigenvalues and (b) the eigenstates from a random chain with $N = 256$ atoms. (c) The sketch diagram of a series of resonance two-level bound states. (d) The laser pulse and (e) the time-dependent population for the resonance states $\phi_1(x)$ and $\phi_{256}(x)$ when the initial state is $\phi_1(x)$.

for different random realizations of the model and then coherently sum all these contributions to the HHG signal to properly account for the intrinsic disorder of the liquid phase. In the numerical simulations, the fundamental driving laser wavelength is $\lambda_0 = 1600$ nm, and the field strength $E_0 = 0.015$ a.u. For the second pulse, $E_{20} = 0.3E_0$, $\lambda_2 = \lambda_0/3$, or $\lambda_2 = \lambda_0/2$ is applied. The phase difference φ is set to be zero. The results are shown in Fig. 1. Since it is a disordered system, the noise floor is high compared to the HHG from ideal atomic and crystal systems. We identify the cutoff energy in the symmetric ω_0 and $\omega_0 + 3\omega_0$ fields by the intensity change and the separation point of the odd- and even-order harmonics. The even harmonics correspond to the fluctuation of the disordered system, which is incoherent and cannot be measured in experiments. From Fig. 1 one can find that the cutoff energy in the monochromatic ω_0 field is around $43\omega_0$. The cutoff energy in the $\omega_0 + 3\omega_0$ fields is around $45\omega_0$. For the $\omega_0 + 2\omega_0$ fields, the cutoff energy is identified by the separation point of stable harmonics and fluctuation harmonics by investigating their intensities with different numbers of random chains. The former is robust, while the latter changes obviously in different chains. One can find that even-order harmonics are generated, and the cutoff energy is $44\omega_0$. The results in $\omega_0 + 2\omega_0$ fields qualitatively agree with the case of $\omega_0 + 3\omega_0$. In the latter it is easy to identify the cutoff energy. Thus we mainly present the $\omega_0 + 3\omega_0$ results next. The strength of the two-color fields is $E' = 1.3E_0$ when $\varphi = 0$. From the cutoff law in monochromatic fields, the cutoff energy is expected to increase 30%. However, the TDSE results in bichromatic fields do not support the linear cutoff law anymore. This phenomenon seems abnormal, which indicates that the second laser field can change the symmetry of the system, but cannot obviously extend the maximum HHG energy. It suggests that the mechanism of liquid HHG is complex. A new theory needs to be established to describe the interactions between intense laser fields and liquids.

III. RESULTS AND DISCUSSION

To analyze the origin of liquid HHG, we calculate the eigenvalues and eigenstates of the random model chain in Ref. [15] by numerically solving the stationary Schrödinger equation. The eigenvalues from the chain with $N = 256$ atoms are shown in Fig. 2(a), and there is a band gap between the bound states and the quasifree states. Figure 2(b) shows four representative wave functions for the cases of $n = 1$, 25, 232, and 256, respectively. One can easily find that the wave functions are localized states, which agrees with the theory of Anderson localization of a disordered system [23]. $\phi_1(x)$ and $\phi_{256}(x)$ are mainly located near the 47th and 48th potentials with the same modulus of the wave function, and the difference is the sign of the wave function for the adjacent potentials. The pair of states $\phi_{25}(x)$ and $\phi_{232}(x)$ has a similar characteristic but is located in the region from the 33rd to 38th potentials. Further verification shows that almost all of the bound states distribute in pairs. This reminds us of the resonance excitation between the ground state and the first excited state in H_2^+ [24]. Figure 2(c) shows the sketch diagram of the resonance between the pairs of the states. They are almost degenerate. The maximum energy difference of bound states is $\Delta\varepsilon_m = 0.0096$ a.u. and it is less than the photon energy of the fundamental field. This is reasonable since the energy shift of one liquid molecule is less influenced by others because of their relatively long intermolecular distance and long-range disorder. The resonance is verified by calculating the time-dependent electron population with the initial state at $\phi_1(x)$ in a laser pulse. Figure 2(d) shows the laser field and Fig. 2(e) shows the electron population on the states $n = 1$ and $n = 256$. The population transfer is almost 100% at some times. The resonance excitation also occurs in other pairs of states as well. As a result, we propose a statistical two-level model and give a physical picture for the HHG in liquids.

From the mathematical derivation [24], the maximum harmonic energy from a pair of strongly coupling states in the

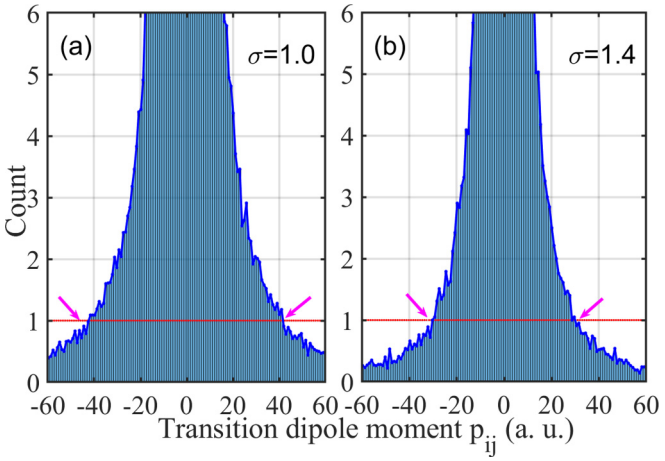

FIG. 3. The statistics of transition dipole moment p_{ij} for different standard deviations: (a) $\sigma = 1.0$, (b) $\sigma = 1.4$. The interval of the dipole is set to be $d_p = \omega_0/(2E_0)$ to make sure the resolution of harmonic energy is one photon. The count is divided by the number of configurations, M.

monochromatic field is

$$\Omega_{\text{cutoff}} = 2p_{12}E_0, \tag{2}$$

where p_{12} is the transition dipole between the resonance states [24]. This can explain the experimentally measured linear dependence of maximum harmonic energy as a function of laser field strength E_0 and the independence of wavelength [15]. By comparing the above equation and Eq. (1), an effective dipole moment p^* should be

$$p^* = \frac{d^*}{2} = \frac{a(a-\sigma)}{2\sigma}. \tag{3}$$

To justify this connection between the dipole and maximum coherence distance d^*, we use $M = 100$ chains with the same statistical parameter σ to make a statistic of the number of p_{ij} between different pairs of resonance states. The count in the y axis of Figs. 3(a) and 3(b) is the total count divided by the number of configurations, M. One can find that the maximum value of $2p_{ij}$ is much bigger than the maximum coherence distance d^* [15]. However, d^* is a statistical distance that stands for the maximum stable coherence. From this sense, $d^*/2$ should correspond to a critical value of p_{ij} that must appear M times in the M configurations. Otherwise, it corresponds to the fluctuation part of the liquid system, which cannot generate stable coherent harmonic signals. In other words, the count of critical p_{ij}^c in Figs. 3(a) and 3(b) should be one. For $\sigma = 1.0$ from our estimation in Eq. (3), $p_{ij}^c = d^*/2 = 45$ a.u. For $\sigma = 1.4$, p_{ij}^c should be 31 a.u. One may find that the estimations agree well with the statistical values in Fig. 3. We can conclude that our statistical resonance model can well explain our TDSE results and the empirical formula (1) in a monochromatic laser field. It provides a connection between the classical and quantum pictures of liquid HHG.

To further justify the model, we can separate the contribution of HHG from different states in the length gauge by projecting the time-dependent wave function on the eigen-

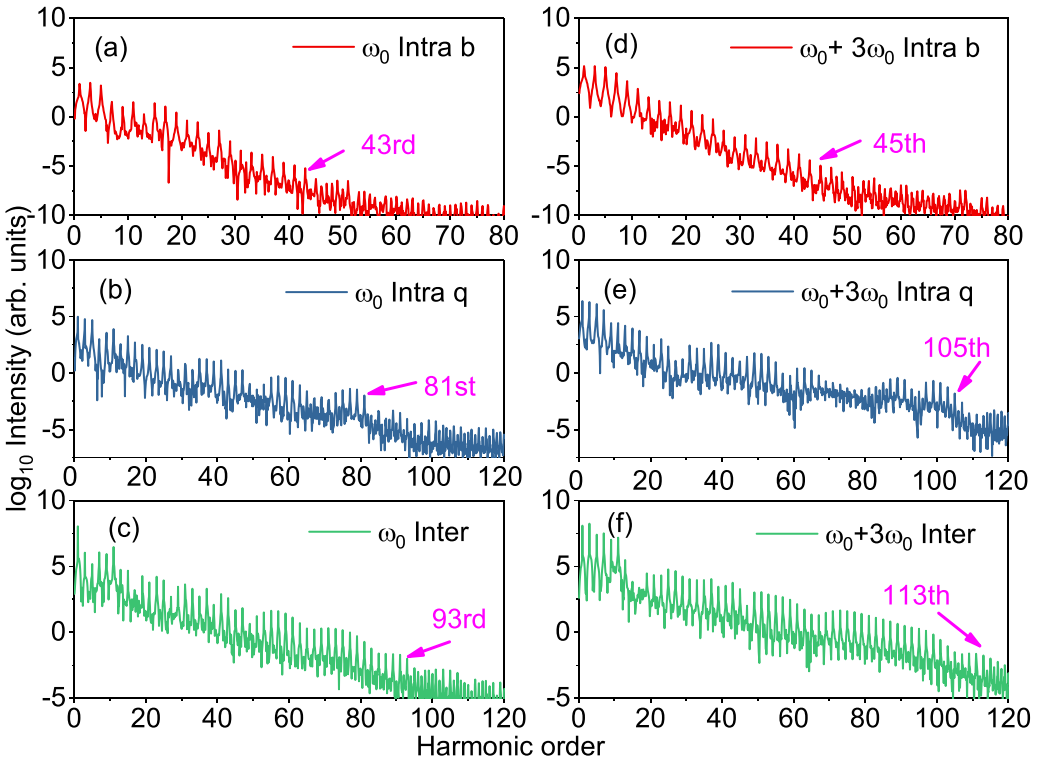

FIG. 4. Intraharmonic spectrum of bound and quasifree states and interharmonic spectrum between them. (a–c) one-color scheme, (d–f) two-color scheme. Intraharmonic spectra for bound states are shown in (a) and (d), intraharmonic spectra for quasifree states are shown in (b) and (e), and interharmonic spectra are shown in (c) and (f). The laser parameters are the same as those in Fig. 1.

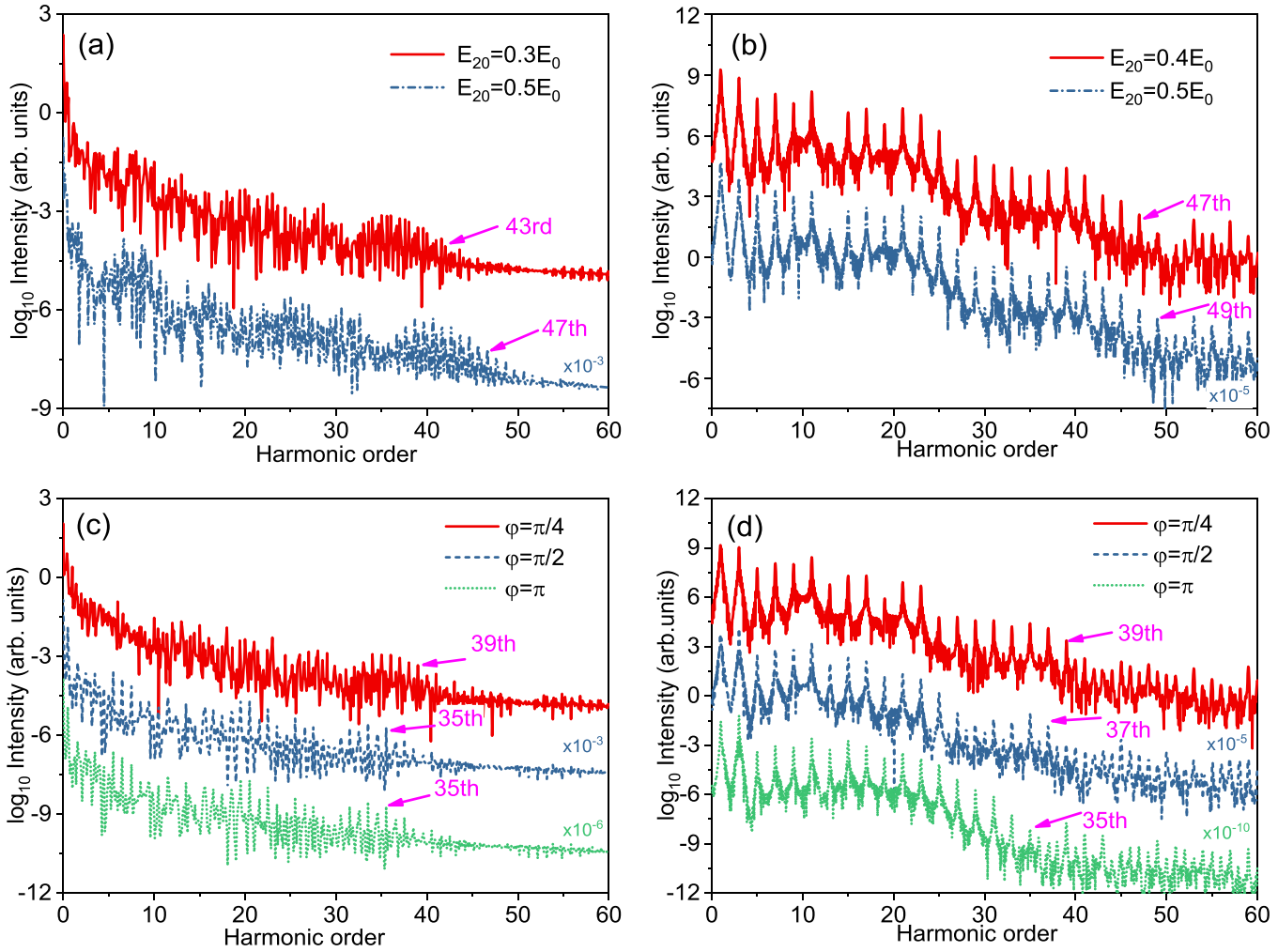

FIG. 5. HHG spectra with different phases and strengths of the second laser: (a, c) obtained by the three-level model and (b, d) TDSE simulations. In (a) and (b), the phase is set to be zero. In (c) and (d), the strength of the second field $E_{20} = 0.3E_0$.

states [25–28]. The intracurrent is given by

$$J_{\text{intra}} = -\langle \Phi^{b(q)}(x,t)|\hat{p}|\Phi^{b(q)}(x,t)\rangle, \tag{4}$$

where b and q stand for the bound states and the quasifree states, $|\Phi^b(x,t)\rangle = \sum_{i=1}^{N} |\phi_i(x)\rangle\langle\phi_i(x)|\psi(x,t)\rangle$ and $|\Phi^q(x,t)\rangle = \sum_{i=N+1}^{2N} |\phi_i(x)\rangle\langle\phi_i(x)|\psi(x,t)\rangle$. The higher states are ignored because of the very low population in the evolution. The intercurrent between quasifree states and the bound states can be obtained by

$$J_{\text{inter}} = -\langle \Phi^{b}(x,t)|\hat{p}|\Phi^{q}(x,t)\rangle. \tag{5}$$

The intraharmonic spectrum for bound resonant states in the one-color scheme is shown in Fig. 4(a); the cutoff is about 43rd, which is equal to the cutoff of the total harmonic spectra shown in Fig. 1. Figure 4(b) shows the intraharmonics from the quasifree states and the cutoff is about 81st. The interharmonic spectrum is also simulated as shown in Fig. 4(c). Only odd orders are obtained and the cutoff is about 93rd order. The intensity of the interharmonics is much higher than others. Those results indicate that the intensity of liquid HHG is determined by the transition between the quasifree state and localized bound states. However, the cutoff energy is determined by the coherence length of the resonant bound states, similar to the cask theory. The whole process can be described as follows: (i) electron coupling in a series of bound resonant two-level localized states with a small displacement and the emission of intra-bound-state HHG; (ii) ionization from the resonance states and movement in quasifree states with a bigger range, leading to intra-quasifree-state HHG; and (iii) transition from quasifree states to resonant bound states with interband HHG emission. Different from the ideal gas and crystal systems, the coherence length or the cutoff energy in disordered liquids is determined by the bound two-level resonance states since they play key roles in the initial and final steps.

For the case of the two-color scheme with $\varphi = 0$, the effective field strength $E' = 1.3E_0$. We give more information in Figs. 4(d)–4(f). The cutoff of the intraharmonics of bound states changes little, even though the cutoff of interharmonics is extended to 113th order, and the cutoff of intraharmonics of quasifree states is extended to 105th order. This implies that the cutoff of total harmonics still depends on the pairs of resonant bound states by the cask theory. The two-color fields can modulate the symmetry of the system during acceleration of the ionized electrons in step (ii), which leads to

the even-order harmonic generation in $\omega_0 + 2\omega_0$ fields. They disappear again in $\omega_0 + 3\omega_0$ fields because the symmetry of the laser fields is restored. However, the two-color field cannot effectively increase the cutoff of HHG from intrabound states.

To further reveal why the cutoff energy of intra-bound-state harmonics is not obviously changed in this case, we have to include the strong coupling between the resonant two states and the continuum states because of the big photon energy of the second field. For simplicity, we use one quasifree state to represent all the other free states. Then the system is reduced to a three-level system. It is difficult to find the analytic solution of this three-level system. We solve it numerically instead. The results are shown in Fig. 5(a). Due to the beating of the three-level states, the structure of the spectra is complex, but it could provide clear cutoff information. One can find that the cutoff energy is slightly changed compared to the calculation of monochromatic fields. It qualitatively agrees with the results in Fig. 1. When we increase the strength of the $3\omega_0$ field, the cutoff energy slightly increases for the case of $\varphi = 0$. It agrees with the TDSE results in Fig. 5(b).

The phase effects in $\omega_0 + 3\omega_0$ fields by the three-level simulations and the TDSE are shown in Figs. 5(c) and 5(d), respectively. The cutoffs by TDSE are 39th, 37th, and 35th for the cases of the phases $\pi/4$, $\pi/2$, and π, respectively, which agrees qualitatively with the three-level simulations. For $\varphi = \pi$, the ω_0 and $3\omega_0$ fields are destructively interfered at $t = nT_0/2$, but they may constructively interfere at other times. The peak strength of the superposed field is still around $0.9E_0$. From the cutoff law in monochromatic fields, the cutoff energy should only decrease 10%. However, Fig. 5(c) by the three-level calculation and Fig. 5(d) by TDSE show an obvious decrease of HHG cutoff energy. It comes from the coupling of quasifree states in two-color fields.

IV. CONCLUSION

In conclusion, the mechanism of HHG from liquid systems is revealed by our statistical resonance model, which can explain the results of TDSE simulations in both the monochromatic and bichromatic laser fields. This is a full quantum picture for the physical mechanism explanation of HHG in bulk liquids. Its validity is justified by the success in interpreting the linear cutoff energy dependence of field strength, and the independence of wavelength in the monochromatic field. By including the coupling to continuum states, the problem of the results in two-color fields is also solved. Our microscopic model will help understand other phenomena in liquid HHG optical sources. It also provides us clues for the optimal control of electron dynamics in liquids, which may be useful in chemical and biological processes.

ACKNOWLEDGMENTS

We thank Z. Yin and H. J. Wörner for the helpful discussions. This work is supported by the National Natural Science Foundation of China (NSFC) (Grant No. 91850121), the K. C. Wong Education Foundation (GJTD-2019-15), the China Postdoctoral Science Foundation (Grant No. 2020M682525), and the Natural Science Foundation of Shanxi Province (Grant No. 201901D111288).

C.L.X., Z.L.L., and J.Q.L. contributed equally to this work.

[1] F. Krausz and M. Ivanov, Rev. Mod. Phys. **81**, 163 (2009).
[2] L. V. Keldysh, Sov. Phys. JETP **20**, 1307 (1965).
[3] N. B. Delone and V. P. Krainov, J. Opt. Soc. Am. B **8**, 1207 (1991).
[4] L. B. Madsen, F. Jensen, O. I. Tolstikhin, and T. Morishita, Phys. Rev. A **89**, 033412 (2014).
[5] A. McPherson, G. Gibson, H. Jara, U. Johann, T. S. Luk, I. A. McIntyre, K. Boyer, and C. K. Rhodes, J. Opt. Soc. Am. B **4**, 595 (1987).
[6] P. B. Corkum, Phys. Rev. Lett. **71**, 1994 (1993).
[7] M. Lein, N. Hay, R. Velotta, J. P. Marangos, and P. L. Knight, Phys. Rev. Lett. **88**, 183903 (2002).
[8] J. Itatani, J. Levesque, D. Zeidler, H. Niikura, H. Pépin, J. C. Kieffer, P. B. Corkum, and D. M. Villeneuve, Nature (London) **432**, 867 (2004).
[9] K. A. Pronin, A. D. Bandrauk, and A. A. Ovchinnikov, Phys. Rev. B **50**, 3473 (1994).
[10] G. Vampa, C. R. McDonald, G. Orlando, D. D. Klug, P. B. Corkum, and T. Brabec, Phys. Rev. Lett. **113**, 073901 (2014).
[11] C. Thaury and F. Quéré, J. Phys. B **43**, 213001 (2010).
[12] A. Flettner, T. Pfeifer, D. Walter, C. Winterfeldt, C. Spielmann, and G. Gerber, Appl. Phys. B **77**, 747 (2003).
[13] A. D. DiChiara, E. Sistrunk, T. A. Miller, P. Agostini, and L. F. DiMauro, Opt. Express **17**, 20959 (2009).
[14] T. T. Luu, Z. Yin, A. Jain, T. Gaumnitz, Y. Pertot, J. Ma, and H. J. Wörner, Nat. Commun. **9**, 3723 (2018).
[15] A. W. Zeng and X. B. Bian, Phys. Rev. Lett. **124**, 203901 (2020).
[16] M. Wu, S. Ghimire, D. A. Reis, K. J. Schafer, and M. B. Gaarde, Phys. Rev. A **91**, 043839 (2015).
[17] G. Vampa, C. R. McDonald, G. Orlando, P. B. Corkum, and T. Brabec, Phys. Rev. B **91**, 064302 (2015).
[18] K. K. Hansen, T. Deffge, and D. Bauer, Phys. Rev. A **96**, 053418 (2017).
[19] C. Yu, K. K. Hansen, and L. B. Madsen, Phys. Rev. A **99**, 063408 (2019).
[20] N. Tancogne-Dejean, O. D. Mücke, F. X. Kärtner, and A. Rubio, Phys. Rev. Lett. **118**, 087403 (2017).
[21] A. D. Bandrauk, S. Chelkowski, H. Yu, and E. Constant, Phys. Rev. A **56**, R2537 (1997).
[22] J. B. Li, X. Zhang, S. J. Yue, H. M. Wu, B. T. Hu, and H. C. Du, Opt. Express **25**, 18603 (2017).
[23] P. W. Anderson, Phys. Rev. **109**, 1492 (1958).
[24] T. Zuo, S. Chelkowski, and A. D. Bandrauk, Phys. Rev. A **48**, 3837 (1993).
[25] Z. Guan, X. X. Zhou, and X. B. Bian, Phys. Rev. A **93**, 033852 (2016).
[26] P. Földi, Phys. Rev. B **96**, 035112 (2017).
[27] R. E. F. Silva, F. Martín, and M. Ivanov, Phys. Rev. B **100**, 195201 (2019).
[28] L. Yue and M. B. Gaarde, Phys. Rev. A **101**, 053411 (2020).